Modulation of optical transmittance and conductivity by the period, linewidth and height of Au square mesh electrodes

Guanghong Yang, Bing Liu, Ke Cheng, and Zuliang Du*

Key Lab for Special Functional Materials of Ministry of Education, Henan University, Kaifeng 475004, China
*zld@henu.edu.cn

Abstract:Metal transparent conductive electrode (TCE) with surface plasmons has been extensively studied for light absorption enhancement in solar cells and light extraction in Light-Emitting Diodes etc. But its transparent conductive properties and surface plasmons are controlled by its micromorphologies and microstructures. In this work, photoelectric coupling effects and optical transmittance modulations of period, linewidth and height of Au nanowire in square mesh electrode were investigated detailedly using a comprehensive finite-difference time domain calculation stimulation, and then Au square mesh TCEs with the 500 nm in period, 70 nm in height and linewidth ranging from 60 to 100 nm were fabricated using electron beam lithography. The measured results showed that the optical transmittance of the TCEs is about 70% in the 350-700 nm wavelength range and over 80% in the 700-1000 nm range, which accord with the theoretical simulation results. Optical transmittance is affected by reflection loss, localized surface plasmon resonances and surface plasmon polarizations (SPPs) absorption loss, concerned about geometry parameters. SPPs dip peak position exhibits a blue-shift from 844 to 812 nm and the width of peak increases with increasing the linewidth from 60 to 100 nm, The measured surface resistivity of the TCEs with the 500 nm in period, 50 nm in height and 50 nm in linewidth is about 74.5 Ω/m^2, about two times bigger than that of commercial indium tin oxide glass.

OCIS codes: (240.6680) Surface plasmons; (310.7005) Transparent conductive coatings; (350.2770) Gratings.

References and links

1. A. R. Madaria, A. Kumar, and C. Zhou, "Large scale, highly conductive and patterned transparent films of silver nanowires on arbitrary substrates and their application in touch screens," Nanotechnology **22**(24), 245201 (2011).
2. S. Coskun, E. S. Ates, and H. E. Unalan, "Optimization of silver nanowire networks for polymer light emitting diode electrodes," Opt. Express **22**(S5), A1372–A1379 (2009).
3. T. S. Luk, N. T. Fofang, J. L. Cruz-Campa, I. Frank, and S. Campione, "Solution-processed metal nanowire mesh transparent electrodes," Nano Lett. **8**(2), 689–692 (2008).
4. S. Kiruthika, R. Gupta, K. D. M. Rao, S. Chakraborty, N. Padmavathy, and G. U. Kulkarni, "Large area solution processed transparent conducting electrode based on highly interconnected Cu wire network," J. Mater. Chem. C **2**(11), 2089–2094 (2014).
5. Z. Chena, B. Cotterell, W. Wang, E. Guenther, and S. J. Chua, "A Mechanical Assessment of Flexible Optoelectronic Devices," Thin Solid Films **394**(1–2), 201–205 (2001).
6. H. J. van de Wiel, Y. Galagan, T. J. van Lammeren, J. F. de Riet, J. Gilot, M. G. M. Nagelkerke, R. H. C. A. T. Lelieveld, S. Shanmugam, A. Pagudala, D. Hui, and W. A. Groen, "Roll-to-roll embedded conductive structures integrated into organic photovoltaic devices," Nanotechnology **24**(48), 484014 (2013).
7. N. Kwon, K. Kim, S. Sung, I. Yi, and I. Chung, "Highly conductive and transparent Ag honeycomb mesh fabricated using a monolayer of polystyrene spheres," Nanotechnology **24**(23), 235205 (2013).
8. L. Ke, R. S. Kumar, P. Chen, L. Shen, S. J. Chua, and A. P. Burden, "Au-ITO Anode for Efficient Polymer Light-Emitting Device Operation," IEEE Photon. Technol. Lett. **17**(3), 543–545 (2005).

#222289 - $15.00 USD Received 2 Sep 2014; revised 7 Nov 2014; accepted 28 Nov 2014; published 16 Jan 2015

9. I. Kim, T. S. Lee, D. S. Jeong, W. S. Lee, W. M. Kim, and K. S. Lee, "Optical design of transparent metal grids for plasmonic absorption enhancement in ultrathin organic solar cells," Opt. Express **21**(S4 Suppl 4), A669–A676 (2013).
10. J. Kholopova, A. Kovalchuk, E. Polushkin, V. Zemlyakov, S. Shapoval, D. Kozlov, I. Khmyrova, T. Hasegawa, and S. Tomioka, "Patterning of Top Metal Electrode for Light Extraction Improvement in Light-Emitting Diodes," in 11th international conference on nanoimprint and nanoimprint technology (2013).
11. C. Cao, J. Zhang, X. Wen, S. L. Dodson, N. T. Dao, L. M. Wong, S. Wang, S. Li, A. T. Phan, and Q. Xiong, "Metamaterials-Based Label-Free Nanosensor for Conformation and Affinity Biosensing," ACS Nano **7**(9), 7583–7591 (2013).
12. Z. Ye, S. Chaudhary, P. Kuang, and K. M. Ho, "Broadband light absorption enhancement in polymer photovoltaics using metal nanowall gratings as transparent electrodes," Opt. Express **20**(11), 12213–12221 (2012).
13. J. A. Schuller, E. S. Barnard, W. Cai, Y. C. Jun, J. S. White, and M. L. Brongersma, "Plasmonics for extreme light concentration and manipulation," Nat. Mater. **9**(3), 193–204 (2010).
14. J. van de Groep, P. Spinelli, and A. Polman, "Transparent Conducting Silver Nanowire Networks," Nano Lett. **12**(6), 3138–3144 (2012).
15. K. Cheng, Z. Cui, Q. Li, S. Wang, and Z. Du, "Large-scale fabrication of a continuous gold network for use as a transparent conductive electrode in photo-electronic devices," Nanotechnology **23**(42), 425303 (2012).
16. S. Xie, Z. Ouyang, B. Jia, and M. Gu, "Large-size, high-uniformity, random silver nanowire networks as transparent electrodes for crystalline silicon wafer solar cells," Opt. Express **21**(S3 Suppl 3), A355–A362 (2013).
17. S. Kiruthika, R. Gupta, K. D. M. Rao, S. Chakraborty, N. Padmavathy, and G. U. Kulkarni, "Large area solution processed transparent conducting electrode based on highly interconnected Cu wire network," J. Mater. Chem. C **2**(11), 2089–2094 (2014).
18. S. Y. Chou, P. R. Krauss, and P. J. Renstrom, "Imprint lithography with 25-nanometer resolution," Science **272**(5258), 85–87 (1996).
19. M. G. Kang and L. J. Guo, "Nanoimprinted Semitransparent Metal Electrodes and Their Application in Organic Light-Emitting Diodes," Adv. Mater. **19**(10), 1391–1396 (2007).
20. M. G. Kang, M. S. Kim, J. Kim, and L. J. Guo, "Organic Solar Cells Using Nanoimprinted Transparent Metal Electrodes," Adv. Mater. **20**(23), 4408–4413 (2008).
21. P. Kuang, J. M. Park, W. Leung, R. C. Mahadevapuram, K. S. Nalwa, T. G. Kim, S. Chaudhary, K. M. Ho, and K. Constant, "A New Architecture for Transparent Electrodes: Relieving the Trade-Off Between Electrical Conductivity and Optical Transmittance," Adv. Mater. **23**(21), 2469–2473 (2011).
22. G. Veronis and S. Fan, "Overview of Simulation Techniques for Plasmonic Devices," in *Surface plasmon nanophotonics*, (Springer, 2007).
23. E. D. Palik, *Handbook of Optical Constants of Solids* (Academic Press, 1985).
24. P. B. Catrysse and S. Fan, "Nanopatterned Metallic Films for Use As Transparent Conductive Electrodes in Optoelectronic Devices," Nano Lett. **10**, 2944–2949 (2010).

1. Introduction

In optoelectronic devices [1–3], metal nanostructures, as a transparent conductive electrode (TCE), have many advantages over Indium tin oxide (ITO) film such as high optical transparency, good electrical conductivity [4], mechanical ⟩exibility [5], easy machining [6,7] and compatibility with the mass production style [8]. Moreover, the cooperative interactions between light and metal nanostructures can produce localized surface plasmon resonances (LSPRs) and surface plasmon polaritons (SPPs), which make metal TCE suitable for light absorption enhancement in the solar cells (SCs) [9], light extraction in the Organic LEDs [10] and biological detection [11] etc. These interactions occur mainly at a range of tens of nanometers and were controlled by the structure size and geometric characteristics significantly [12,13], optical transmittance could be modulated by diffraction coupling, the cutoff of fundamental transverse electric propagating mode, LSPRs and SPPs [9,14]. Inappropriate designs always bring about low transmittance and resistive losses, which affect the device performances. Therefore, fine tuning is essential because of the trade-off between optical transmittance and conductivity to develop high-performance TCEs with many advantages.

Many methods, such as nanosphere lithography [15], metal nanowires liquid phase dispersion method [16] and thin film crack template [17], are adopted to achieve metal TCEs. However, it is difficult to finely adjust optical transmittance, conductivity and photoelectric coupling using the above-mentioned methods due to random distribution of metal nanowires, uncontrollable mesh size, and the limited abilities in the fabrication precision, flexibility and

#222289 - $15.00 USD Received 2 Sep 2014; revised 7 Nov 2014; accepted 28 Nov 2014; published 16 Jan 2015

adjustment to linewidth. Nanoimprint lithography (NIL) method can achieve high-output, high precision replication of the nanostructures according to the ordered structure and linewidth characteristics of stamps [18], The Au, Cu and Al TCEs were fabricated using the NIL method [19,20], high optical transmittance and small surface resistivity have been obtained, which is close to the level of ITO films. One dimensional (1D) Au and Ag nanotape were fabricated using polyurethane grating template with the 2.5 μm in periodicity, 40 nm in linewidth and 1.2 μm in height, and their optical transmittance reached 80% and the surface resistivity of Au and Ag electrodes were respective 9.7 and 3.2 ohm/m2, better than that of ITO films [21]. Electron beam lithography (EBL), as a powerful patterning tool with excellent resolution, was often used to fabricate hyperfine nanostructures [13]. The transparent conductive properties of Ag square mesh TCEs had been by EBL fabrication in experiment and the desired high-performance predicted by calculational simulation had been obtained [14].

Compared with the Cu and Ag electrodes, Au electrodes have the advantages of high work function and antioxidation in the applications to organic LEDs and SCs [8,12]. Relatively few reports mentioned only transparent properties of Au square mesh TCEs [19,20], photoelectric coupling and its effects on transmittance still lack detailed investigates. In this letter, photoelectric coupling effects and optical transmittance modulations of period, linewidth and height of Au nanowire in square mesh electrode was analyzed detailedly by electrodynamic simulations using a comprehensive 2D finite-difference time domain (FDTD) calculation, and Au square mesh electrodes were fabricated by using the EBL method and their transparent conductive properties accord with the simulated results, which will provide some references for the designs of Au TCEs.

2. Experimental methods

2.1. Optimization of the nanowire period, linewidth and height of Au TCEs

Optimization of the nanowire period, linewidth and height in Au TCEs was made by the electrodynamic analysis using the FDTD method [22]. A plane wave is used as source. The Poynting vector behind the electrode is monitored and normalized to incidence wave. Perfectly matched layers are used in the incidence direction, anti-symmetric and symmetric boundaries conditions are used in both edges in directions parallel and vertical to the E-polarization, respectively. Gold parameters were modeled as Lorentz-Drude dielectric functions using the method of Palik et al [23].

2.2. Fabrication of the Au square mesh electrodes

The square mesh electrode nanopattern was designed by Nanopattern Generator made by the Institute of electrical engineering, Chinese Academy of Sciences. Au square mesh electrodes were fabricated on Si wafer with a SiO_2 layer in 200 nm thickness as the electric insulation layer to allow electrical measurement. Firstly, silicon wafers and ITO films were cleaned ultrasonically in deionized water, ethanol and acetone in sequence, and then dried by Nitrogen. Secondly, a layer of polydimethylglutarimide (PMGI) SF5 and Polymethylmethacrylate (PMMA) was spin-coated in turn on silicon wafer at the speed of 4000 revolutions per minute (rpm), and then baked at 180°C for 5 minutes or 30 min on a contact hot plate. Focused electron beam on the JSM 5600 scanning electron microscope was controlled to write in PMMA films corresponding to the designed patterns. The expose doses were varied between 1060 and 1500 pC/cm to obtain nanogrooves with different linewidths. The exposed PMMA samples were developed imaging in the mixed solvent of methylisobutylketone and isopropanol (1:3), and then PMGI SF5 being developed imaging in 1% deionized water solvent of tetramethylammonium hydroxide. The Au film was magnetron-sputtered and the bilayers of PMMA and SF5 were lifted off in acetone and N-

#222289 - $15.00 USD Received 2 Sep 2014; revised 7 Nov 2014; accepted 28 Nov 2014; published 16 Jan 2015

Methylpyrrolidone in turn, leaving only Au nanostructured electrodes. Detailed informations and resulting electrode patterns are shown in Figs. 1(a)-1(h).

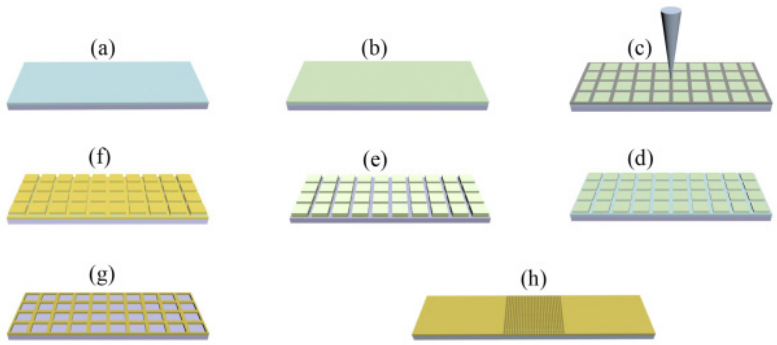

Fig. 1. Fabrication procedures of the Au square mesh electrode. (a) Si wafer is coated with PMGI SF5 and baked at 180 °C for 5 min. (b) SF5/Si is coated with PMMA and baked at 180 °C for 30 min. (c) Electron beam exposure is done. (d) Develop imaging PMMA in the mixed solvent of MIBK and IPA (1:3). (e) Develop imaging SF5 in 1% deionized water solvent of TMAH. (f) Deposition of the Au film. (g) Lift-off bi-layer resist stack, leaving only Au square mesh electrodes. (h) Shows the schematic layout of the resulting sample.

3. Results and discussion

3.1 Optimization of the structural parameters and analysis

Figure 2(a) shows the transmittance and absorption as a function of wavelength in the 400-700 nm range for Au square mesh with the 100 nm in linewidth, the 50 nm in height and different periods. The optical transmittance exceeds 80% in the wavelength larger than 690 nm for the Au square mesh electrodes with different periods. For the Au square mesh with short period, transmittance decreases in the long wavelength without the obvious absorption in the absorption spectrum, which is due to the high coverage of Au. Low optical transmittance in the 300-600 nm ranges for Au square meshes is attributed to the excitations of LSPR, Au nanowire vertical to the polarization of electric field is affected to produce oscillations absorption of free electrons resulting in 50-60% of optical transmittance.

#222289 - $15.00 USD Received 2 Sep 2014; revised 7 Nov 2014; accepted 28 Nov 2014; published 16 Jan 2015

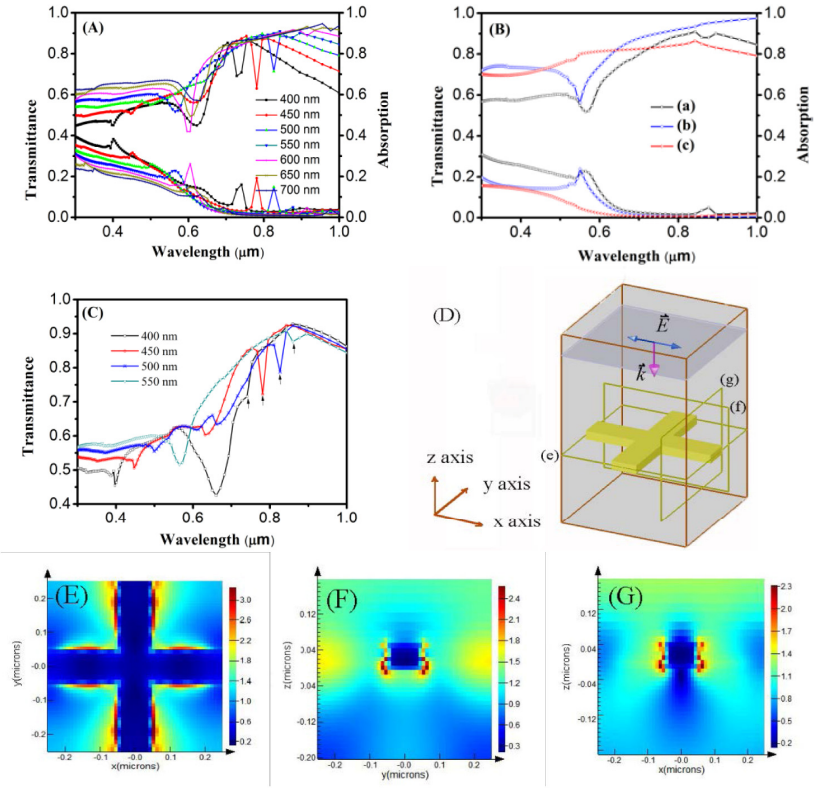

Fig. 2. (A) Simulated optical transmittance (the upper curves) and absorption (the lower curves) as a function of wavelength for a range of periods with 100 nm in linewidth and 50 nm in height; (B) Transmittance (the upper curves) and absorption (the lower curves) as a function of wavelength for the 2D Au nanowire square meshes (a), one nanowire vertical to the polarization direction of electric field (b) and one nanowire parallel to the polarization direction of electric field (c), Period = 550 nm, linewidth = 100 nm, height = 50 nm. (C) Transmittance as a function of wavelength for the Au nanowire square meshes with the 550 nm period in the y direction and the periods in the 400-550 nm range in the x direction. (D) shows the schematic configurations of electric field monitors; $\vec{k}$ denotes light incident direction along the negative Z axis; $\vec{E}$ denotes polarization direction of electric field; the (e), (f) and (g) monitors record electric field profiles in the x-y plane at half height of Au nanograting, in the x-z and y-z planes at 150 nm location apart from the crosspoint, respectively. (E), (F) and (G) present the corresponding electric field profiles in (e), (f) and (g) monitors.

A sharp small transmittance dip occurs at the wavelength equaling to period corresponding to an absorption peak in absorption spectrums, which is owing to the Rayleigh anomaly. At wavelength = period, the ± 1diffraction orders are scattered parallel to the side of nanowires, which result in the strong collective excitation of LSPR modes and strong absorption of light in the Au nanowires. At wavelength larger than period, the excitation of ± 1diffraction make the light transmit directly into substrates, giving rise to slight increase of optical transmittance, but in the 500-700 nm period range, this increase of optical transmittance is counteracted by large transmittance dip from strong reflection. It can be seen that slight transmittance dip and small absorption peaks occur at about 350 nm and 325 nm due to the excitation of ± 2 diffraction for the Au square mesh.

A sharp transmittance dip peak is observed in the range of 700-1000 nm and the peak position shows a red-shift with increasing the period. In order to distinguish the origin of the

#222289 - $15.00 USD Received 2 Sep 2014; revised 7 Nov 2014; accepted 28 Nov 2014; published 16 Jan 2015

peaks, the detailed FDTD calculations were made on solo nanowires vertical and parallel to polarization direction of electric field. Figure 2(b) presents transmittance (upper curves) and absorption (lower curves) spectrums of 2D Au square mesh (a), solo nanowires vertical (b) and parallel (c) to polarization direction of electric field. We can see that only 2D Au nanowire square mesh electrode has an absorption peak in long wavelength range, which is thought as SPPs by Groep [14]. In transmittance of the nanowire perpendicular to the electric field, no SPPs dip peak appears due to the lack of a propagating path in the direction parallel to the electric field. At 550 nm, an evident dip is originating from strong absorption due to Rayleigh anomaly. However, in transmittance of the nanowire parallel to the electric field, this kind of strong absorption doesn't occur except for a broad LSPR absorption band in short wavelength. Figure 2(c) shows the red-shift of SPPs absorption dips with the period variation from 400 nm to 550 nm in direction parallel to the electric field polarization and with the fixed 550 nm period in another direction, as the arrows denote. It is obvious that the red-shift of SPPs dip peaks is mainly due to the lengthened period in direction parallel to the polarization of electric field. The Au nanowire perpendicular to the electric field component of incoming light act as a grating to provide the in-plane momentum required to support a SPP propagating in the direction parallel to the electric field component [14]. Au nanowire parallel to the E polarization direction provides the propagation of SPPs with a path. In the same coupler power conditions, longer propagation path has smaller electronic resistance potential concerned on electron distribution density, the SPPs excited by low energy photon more easily surmount the potential barrier to propagate along Au nanowire.

In order to understand photoelectric coupling of Au square mesh TECs, we set three monitors to get electric field distribution profiles, as shown in Figs. 2(d). the (e), (f) and (g) monitors record electric field profiles in the x-y plane, in the x-z and y-z planes, respectively. Figures 2(e)-2(g) show the corresponding electric field distribution profiles. It can be seen that electric field are mainly condensed on sides and corners of Au nanowires, light-metal nanowire interactions induce electron density distribution on sides and corners, and also the propagation of SPPs is along the sides of Au nanowire.

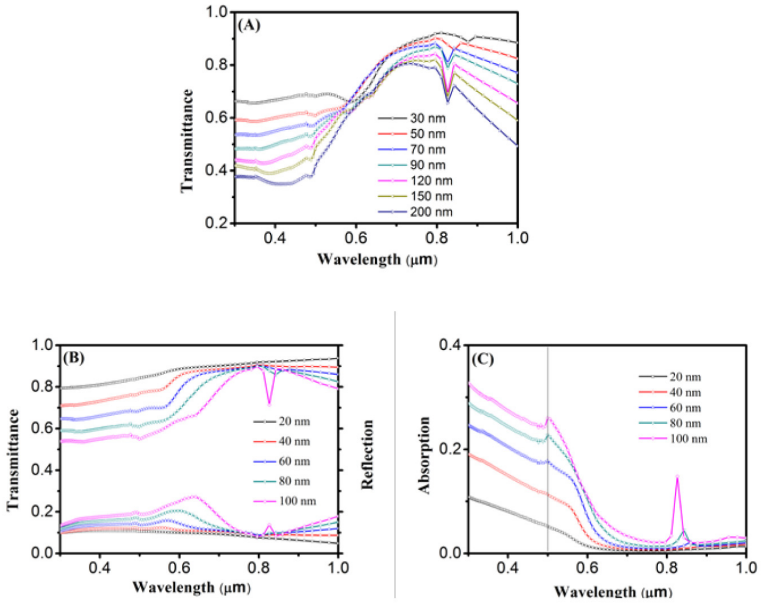

Fig. 3. (A) Simulated optical transmittance as a function of wavelength for a range of heights with 500 nm in period and 80 nm in linewidth; (B) and (C) is the respective simulated transmittance (the upper curves), reflection (the lower curves) and absorption as a function of wavelength for a range of linewidths with 500 nm in period and 50 nm in height.

#222289 - $15.00 USD Received 2 Sep 2014; revised 7 Nov 2014; accepted 28 Nov 2014; published 16 Jan 2015

In Fig. 2(a), a large transmittance dip in the 550-700 nm range is shown for the Au nanowire square mesh with different periods due to reflection, but no obvious dip appears for the Au nanowire square mesh with the 500 nm period. Taking into account the power distribution of solar spectrum, the 500 nm in period is adopted to optimize the height and linewidth of nanowires. As shown in Figs. 3(a) and 3(b), optical transmittance, reflection and absorption as a function of wavelength varies with the heights and linewidths of Au nanowire respectively. With the height increasing from 30 to 200 nm, optical transmittance decreases gradually for wavelengths above 650 nm due to the cutoff of the TE_0 mode according to the modal dispersion calculation [24]. The cutoff is better pronounced with the longer waveguide length (the wire height) in the normal direction showing the waveguide filter performance.

With increasing the height and linewidth, the blue-shift of SPPs dip peak is observed in long wavelength. Based on electric field distribution of nanowire in Fig. 2(e), electric field are mainly enhanced on sides and corners of Au nanowires, for Au nanowire with a larger linewidth and higher height, the SPPs mode is less weakly bound at these positions resulting in lower effective mode index [14], which explains the blue-shift of the SPP peaks with the increasing linewidth of Au nanowire. On the other hand, a bigger linewidth leads to an increase in the scattering cross section of the electrodes so that light can couple more efficiently to the SPP mode and induces the absorption loss, which explains a larger absorption peak for the electrode with a bigger linewidth, as shown in Fig. 3(c). A red-shift of transmittance dip in the 300-500 nm range is observed with the increasing linewidth and height in Figs. 3(a) and 3(b) and corresponds to a red-shift of absorption peak in Fig. 3(c), which is attributed to the LSPR absorption. For metal nanowire electrode with a larger linewidth, the LSPR is more easily excited by lower energy electromagnetic wave owing to the reduced restoring force on the local oscillating electrons, so the red-shift of absorption dip peak occurs in the transmittance spectrum.

A weak transmittance dip at 630 nm in Fig. 3(b) occurs and corresponds to high reflectance, and no obvious absorption peak appears in Fig. 3(c) at the same peak position. So it is concluded that the dip at 630 nm results from the increasing Au coverage leading to high reflectance for Au square mesh electrode with a larger linewidth.

3.2. The morphologies of Au square mesh electrodes

Based on the FDTD calculation analysis, Au square mesh TCEs with the 500 nm in period, 40 nm in linewidth and 50 nm in height has about 80% of optical transmittance. These parameters are adopted to fabricate Au square mesh electrode by the EBL method. Figures 4(a) and 4(b) are the respective morphological images of the Au square mesh TCEs and the contact zone between the pad and the electrode with the period in 500 nm. We can see that the Au square mesh TCEs show the uniformity of the network over a large area and the nanowire linewidth is about 50 nm except for the discharge effect of the edges because of electron scattering during the SEM photograph.

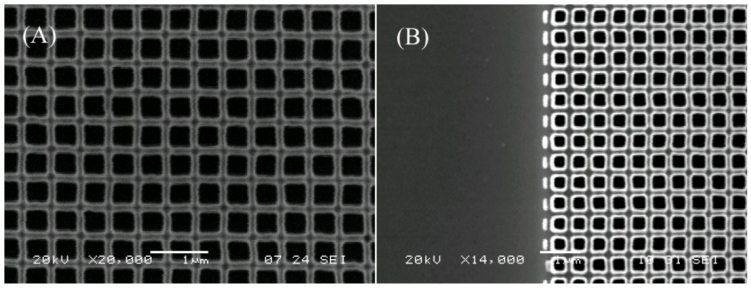

Fig. 4. (A) The SEM image of the Au square mesh electrode with the 500 nm in period, 50 nm in linewidth and 50 nm in height. (B) The SEM image shows the contact zone of the electrode network and the measurement pad.

#222289 - $15.00 USD Received 2 Sep 2014; revised 7 Nov 2014; accepted 28 Nov 2014; published 16 Jan 2015

3.3. The measured optical transmittance of Au square mesh electrodes

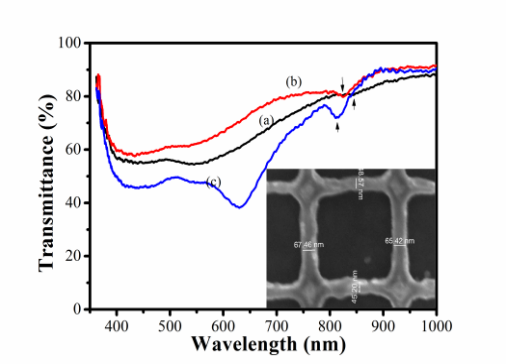

Fig. 5. The measured optical transmittance of the Au square mesh TCEs with the 500 nm in period, 50 nm in height and the linewidths of 60 nm, 65 nm and 100 nm for Curve (a), (b) and (c), respectively. The inset shows SEM image of Au square mesh electrode with the average 60 nm in linewidth.

Figure 5 shows the measured optical transmittance of the Au square mesh TCEs with the 500 nm in period, 50 nm in height and various linewidths ranging from 60 to 100 nm. The weak and broad transmittance dip in the range of 400-550 nm wavelength range belongs to the LSPR absorption based on the FDTD calculation analysis. A red-shift of transmittance dip occurs with the increasing linewidth, which accords with the FDTD calculation analysis. A transmittance dip at 630 nm is resulting from strong reflection in for Au square mesh TCEs with the 100 nm in linewidth. A transmittance dip appears at about 820 nm, which belongs to the SPPs. With the linewidth increasing from 60 to 100 nm, the SPP peak exhibits a blue-shift from 844 nm to 812 nm and the peak area becomes larger, which confirm what the FDTD calculation analysis predict perfectly. It can be found that the transmittance of the electrode with the 60 nm in linewidth be lower than that of the electrode with the 65 nm in width, which might be due to the imperfect liftoff of Au films in the fabrication process.

3.4 The conductive properties of the Au square mesh TCEs

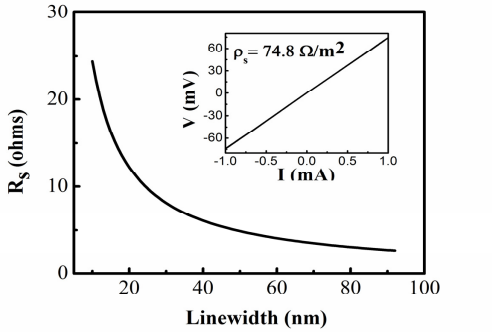

Fig. 6. The surface resistance as a function of nanowire linewidths for Au square mesh electrodes with the 500 nm period and the 50 nm height; The inset shows the I-V curve of the electrode with the 500 nm in period, the 50 nm in linewidth and the 50 nm in height and the corresponding surface resistivity is 74.5 Ω/m^2.

According to Kickoff's law, the sheet resistance (R_s) for the square mesh electrodes with N × N nanowires is given by $R_s = \frac{N}{N+1} R_{nanowire} = \frac{N}{N+1} \frac{\rho L}{wh}$, Where **ρ** is the bulk resistivity of Au (2.44×10^{-8} Ω m at 20°C), **L** is the length of the nanowire period, **w** is the nanowire linewidth

#222289 - $15.00 USD Received 2 Sep 2014; revised 7 Nov 2014; accepted 28 Nov 2014; published 16 Jan 2015

and h is the height of the nanowire. When **N** is larger than 50, the first term is close to unity, such that $\mathbf{R_s}$ equals to $\boldsymbol{\rho L/wh}$. Here **L** equals to 500 nm and **h** equals to 50 nm, we get the relations between $\mathbf{R_s}$ and **w**, $\mathbf{R_s} = 244/\mathbf{w}$. For the square mesh electrode, surface resistivity ($\boldsymbol{\rho_s}$) equals to R_s. Figure 6 shows the $\boldsymbol{\rho_s}$ as a function of linewidths for Au square mesh electrodes with the 500 nm in period and 50 nm in height. It can be seen that the $\boldsymbol{\rho_s}$ decreases from 24.5 to 2.7 ohm/m^2 as the linewidth of TCEs increases from 10 to 92 nm, which are below that of commercial ITO glass (36 ohm/ m^2, 150 nm thickness). The inset shows the measured I-V curve for the Au square mesh TCEs with 50 nm in linewidth and 50 nm in height, and the corresponding $\boldsymbol{\rho_s}$ is 74.5 ohm/m^2, about two times bigger than that of commercial ITO glass and higher than the theoretical value (5.4 ohm/m^2), which may be attributed to compactness, local discontinuities in the nanowires. Au films sputtered at low power own the worse compactness resulting in lower conductivity and improper lift-off of bi-layer resists stack brings about local discontinuities in Au square mesh electrode.

4. Conclusions

The effects of the period, linewidth and height of Au nanowires on the optical transmittance are analyzed using FDTD method. With periods increasing from 400 to 700 nm, optical transmittance increases in the long wavelength range and the ± 1, ± 2 orders diffraction peaks red-shifts occur. With the increasing height from 10 to 200 nm, the optical transmittance in the long wavelength range is affected by the cutoff of the TE_0 mode and decrease rapidly. The Au square mesh TCEs with the 500 nm in period, 70 nm in height and 60 to 100 nm in linewidth were fabricated using the EBL method. The measured optical transmittance is about 70% in the wavelength range of 300-700 nm and over 80% in the 700-1000 nm range, which accord with the theoretical simulation results. SPPs dip peak appears and the peak position shows a blue-shift from 844 to 812 nm and the width of peak increases with increasing the line-width from 60 to 100 nm, which is concerned about the increase of the SPPs required excitation photon energy and the coupling cross-section between light and metal nanostructures. The measured surface resistivity of the electrodes with the 500 nm in period, 50 nm in height and 50 nm in linewidth is about 74.5 ohm/m^2, about two times bigger than that of commercial ITO glass due to preparation drawbacks. This work provides some references for the designs of metal TCEs.

Acknowledgments

This work was supported by Program for Changjiang Scholars and Innovative Research Team in University (No. PCS IRT1126), the National Natural Science Foundation of China (Nos. 11274093, 61376061, and 61240053), the Innovation Scientists and Technicians Troop Construction Projects of Henan Province (No. 114200510015). We would like to give special thanks to Prof. Wei Hu and M. S. Shijun Ge, in Liquid Crystal and Nano-photonics Group, Nanjing University, China for the helps of the microzone optical transmittance measurement.

#222289 - $15.00 USD Received 2 Sep 2014; revised 7 Nov 2014; accepted 28 Nov 2014; published 16 Jan 2015